MODELING AND SIMULATION - A LANE KEEPING ASSIST STUDY

M. Bröcker[1]
[1]TRW Automotive GmbH, Düsseldorf, Germany

Corresponding Author: M. Bröcker, TRW Automotive GmbH, Technical Center Düsseldorf, Global R&D
Hansaallee 190, 40547 Düsseldorf, Germany; markus.broecker@trw.com

Abstract. In this contribution the mathematical modeling of a vehicle equipped with a lane keeping assistance system is considered. Therefore, the modeling considers the steering model of the vehicle and the vehicle itself as a bicycle model. The paper deals for the first time with the mathematical interaction of a driver model in dependence on the situation if the driver does actively steer or not. The lane keeping assist task can be introduced to the driver as a trapezoid overlay torque or as a continuous operating lane guidance controller. Therein, the two lane keeping assist approaches are implemented in a simulation model and a simulation study compares the two approaches.

1 Introduction

Vehicle routes that are marked by long and monotonous driving situations lead to decreasing attention of the driver. Nearly 14 % of all sole accidents with injured persons go back to driving situations where the vehicle leaves the lane. Driver assistance systems and especially the lane keeping assist task can help in reducing these accidents by a correcting steering intervention. This correcting steering intervention is executed for example by an electric motor that is mounted at the steering column of the vehicle. The electric motor executes an overlay torque that can be introduced to the driver as a trapezoid overlay torque or as a continuous operating lane guidance controller.

In this contribution the mathematical modeling for the lane keeping assist task is derived. The modeling contains the vehicle, the steering system and the situation model for the driver interaction. The external rack force couples the vehicle model and the steering model. In a simulation study two control approaches are compared and specific driving manoeuvres on specific road tracks show the working method of each approach.

2 Mathematical modeling for lane keeping

For the lane keeping assist task the vehicle and the steering system are modeled. The vehicle is modeled as a bicycle model, known from e.g. [1,3,4,5], which is sufficient for a lane keeping assist task. The steering system of the car is modeled in this paper by an electro-hydraulic power assist rack and pinion steering gear. In order to overlay a lane keeping assist torque, an electric motor is fitted to the steering column (see figure 1). Alternatively, an electro-mechanical steering system can overlay the lane keeping torque in todays passenger cars [2].

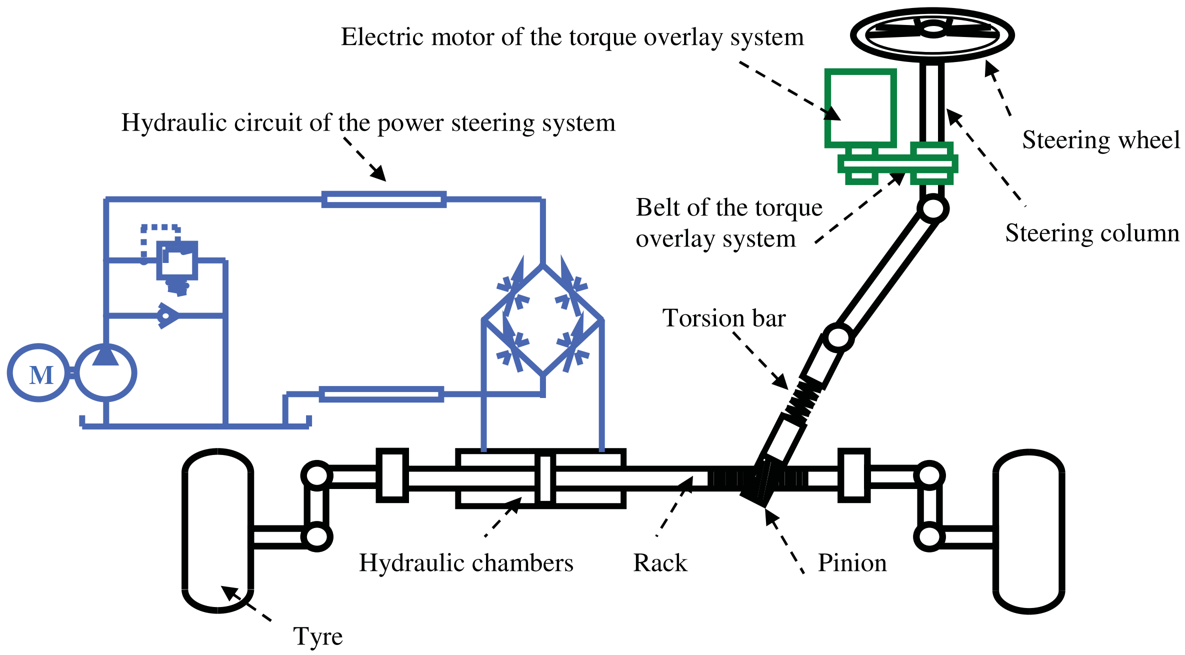

Figure 1. Electric motor at the steering column for the lane keeping assist torque overlay.

For these electro-mechanical steering systems the hydraulic hoses and hydraulic chambers become unnecessary and therefore the electric motor (mounted to the rack or steering column) provides both, the power assist torque and the lane keeping overlay torque. The lane keeping assist task in steer-by-wire steering systems, where the mechanical connection from the steering column is interrupted, is the objective of investigations e.g. in [7].

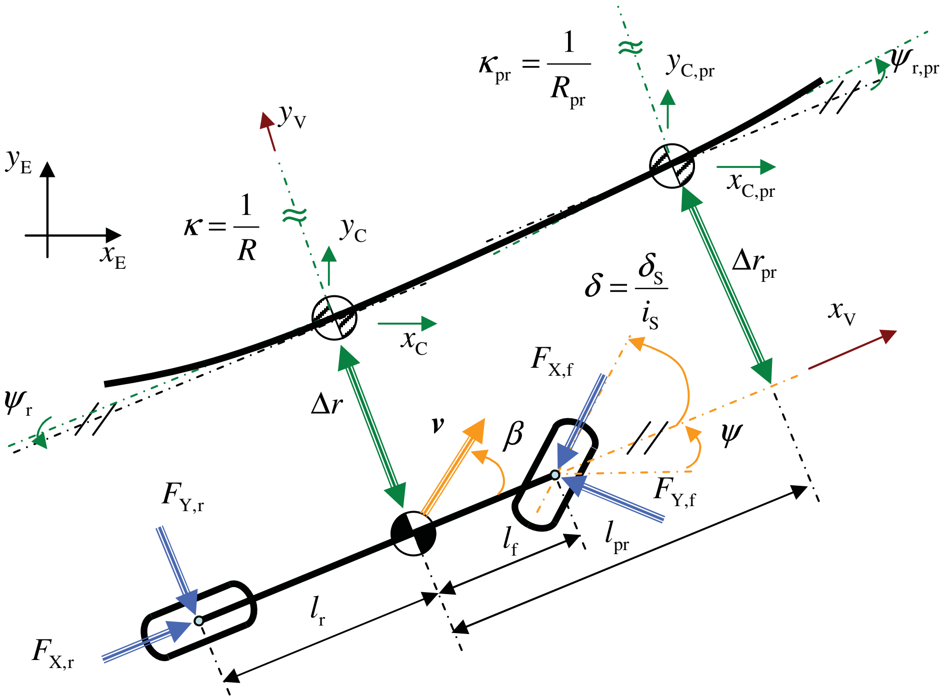

Figure 2. Modeling the vehicle dynamics and the vehicle motion relative to the reference road trajectory.

The vehicle is located in the lane as shown in figure 2. With the world coordinate system (x_E , y_E), the vehicle coordinate system (x_V , y_V) and the reference road trajectory coordinate system (x_C , y_C), the lateral dynamics are fully defined. The bicycle model is determined by two degrees of freedom, the side slip angle β and the vehicle yaw angle ψ . The input signals for the vehicle model are the vehicle speed v_x and the steering wheel angle δ_S (the steering wheel angle δ_S is divided by the steering gear ratio i_S to the steering angle δ). The transfer function for the yaw angle reads as

$$G_\psi(s) = \frac{1}{s}\frac{\dot{\psi}(s)}{\delta(s)} = \frac{1}{s}\left(\frac{\dot{\psi}}{\delta}\right)_{\text{stat}} \cdot \frac{1 + T_1 s}{1 + \frac{2\sigma}{\omega_0^2}s + \frac{1}{\omega_0^2}s^2} \tag{1}$$

with

$$\left(\frac{\dot{\psi}}{\delta}\right)_{\text{stat}} = \frac{1}{l} \cdot \frac{v_x}{1 + \left(\frac{v_x}{v_{ch}}\right)^2}, \tag{2}$$

$$T_1 = \frac{m v_x l_f}{C_r l}. \tag{3}$$

Here, the linear lateral tyre forces $F_{y,f} = C_f \alpha_f$ and $F_{y,r} = C_r \alpha_r$ are considered (with the front and rear tyre slip angle α_f and α_r plus the front and rear cornering stiffness C_f and C_r). The characteristic vehicle velocity is defined by

$$v_{ch} = \sqrt{\frac{l^2 C_f C_r}{m(C_r l_r - C_f l_f)}}. \tag{4}$$

The constant values for the vehicle model are given by the vehicle mass m, the vehicle inertia I_z around the yaw axis, the distances l_f and l_r from the centre of gravity of the vehicle to the front and rear axle and the wheel base $l = l_f + l_r$. The characteristic vehicle speed v_{ch}, the decay constant

$$\sigma = \frac{1}{2} \frac{m\left(C_f l_f^2 + C_r l_r^2\right) + I_z\left(C_f + C_r\right)}{I_z m v_x} \tag{5}$$

and the undamped natural frequency

$$\omega_0 = \sqrt{\frac{C_f C_r l^2 + m v_x^2 \left(C_r l_r - C_f l_f\right)}{I_z m v_x^2}} . \tag{6}$$

determine the stability and the self-steering response of the vehicle. The transfer function for the side slip angle reads as

$$G_\beta(s) = \frac{\beta(s)}{\delta(s)} = \left(\frac{\beta}{\delta}\right)_{\text{stat}} \cdot \frac{1 + T_2 s}{1 + \frac{2\sigma}{\omega_0^2} s + \frac{1}{\omega_0^2} s^2} \tag{7}$$

and

$$\left(\frac{\beta}{\delta}\right)_{\text{stat}} = \frac{l_r}{l} \cdot \frac{1 - \frac{m l_f}{C_r l_r l} v_x^2}{1 + \left(\frac{v_x}{v_{ch}}\right)^2} , \tag{8}$$

$$T_2 = \frac{I_z v_x}{C_r l_r l - l_f m v_x^2} . \tag{9}$$

The output signal from the vehicle model feeds as input signal the steering system model. The external rack force $F_{\text{Ext,Rack}}$ is chosen as output signal from the vehicle model and the computation of the external rack force is defined by

$$F_{\text{Ext,Rack}} = C_f \frac{n_C}{i_S i_P} \left(\delta - \beta - l_f \frac{\dot{\psi}}{v_x} \right). \tag{10}$$

The additional constants the castor n_C (the castor is the sum of constructive and dynamic castor) and the pinion gear ratio i_P have to be taken into account for appropriate modeling. The steering system is modeled by an electro-hydraulic power assist rack and pinion steering gear as shown in figure 3 and figure 4. The mathematical formulation for the steering model is derived in a first step by the differential equation for the translational rack position x_{Rack} (see figure 3) that is given by

$$\ddot{x}_{\text{Rack}} = \frac{1}{m_{\text{Rack}}} \left(\frac{T_{TB}}{i_P} + \frac{i_B T_{EM}}{i_P} + F_A - F_{\text{Ext,Rack}} - F_F \right). \tag{11}$$

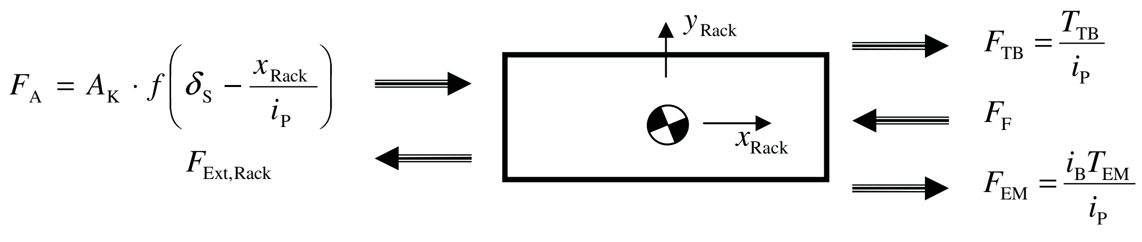

Figure 3. Modeling the rack dynamics.

Here, the rack mass m_{Rack} and the belt gear ratio i_{B} are considered. The torsion bar torque equals $T_{\mathrm{TB}} = c_{\mathrm{TB}}\left(\delta_{\mathrm{S}} - \frac{x_{\mathrm{Rack}}}{i_{\mathrm{P}}}\right) + d_{\mathrm{TB}}\left(\dot{\delta}_{\mathrm{S}} - \frac{\dot{x}_{\mathrm{Rack}}}{i_{\mathrm{P}}}\right)$. The electric motor torque T_{EM} represents the command signal for the closed loop behavior. The assist force F_{A} from the power steering is a nonlinear function $F_{\mathrm{A}} = A_{\mathrm{K}} \cdot f\left(\delta_{\mathrm{S}} - \frac{x_{\mathrm{Rack}}}{i_{\mathrm{P}}}\right)$ with the piston area A_{K}. Additionally, friction at the rack is in existence and therefore the friction force F_{F} has to be modeled e.g. by the rack velocity dependent Stribeck friction.

In a secondary step the modeling of the steering wheel dynamics is derived as shown in figure 4. With the differential equation for the steering wheel angle δ_{S}

$$\ddot{\delta}_{\mathrm{S}} = \frac{1}{I_{\mathrm{S}}}\left(T_{\mathrm{D}} - T_{\mathrm{TB}} - T_{\mathrm{F}} - d_{\mathrm{S}}\dot{\delta}_{\mathrm{S}}\right) \tag{12}$$

the steering system model is fully defined.

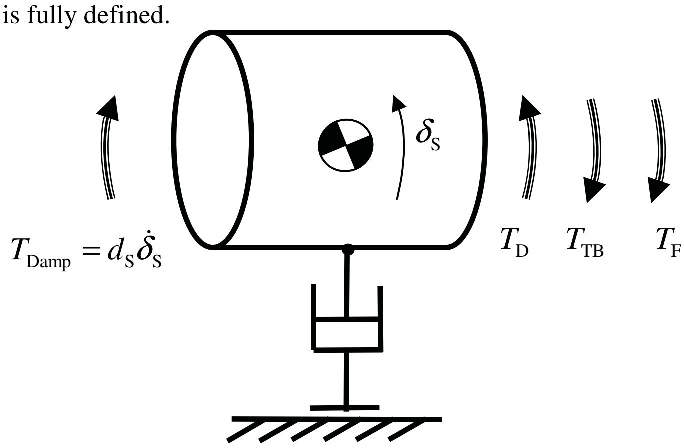

Figure 4. Modeling the steering wheel dynamics.

The constant values for the steering wheel dynamics are given by the steering wheel inertia I_{S} and the steering wheel damping d_{S}. The friction at the steering wheel T_{F} can be modeled with the Stribeck friction in the same manner as the rack friction. The driver torque T_{D} is derived as output from the situation model. This situation model deals with the interaction of a driver model in dependence on the situation if the driver does actively steer or not.

In figure 5 the block diagram for the situation model of the driver interaction is demonstrated. If the driver does actively steer, a significant torsion bar torque T_{TB} appears due to the mechanical torsion bar twist. This torsion bar twist is caused mainly by the difference of the assist force F_{A} from the power steering, the manual steering excitation of the driver and the external rack force $F_{\mathrm{Ext,Rack}}$ from the vehicle. If the driver does actively steer, this situation is referred to the “hands on” situation. Whereas, if the driver releases the hands from the steering wheel and does not actively steer, this situation is referred to the “hands off” situation. For the study of lane keeping assist and lane guidance tasks it is important to distinguish between both situations. Therefore, the situation model is configured as follows.

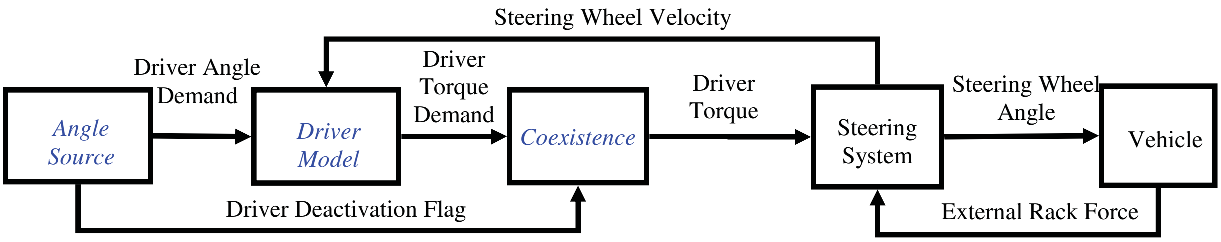

Figure 5. Situation model for the driver interaction: *Angle Source*, *Driver Model* and *Coexistence*.

The situations “hands on” and “hands off” for the driver interaction are basically modeled by the subsystems *Angle Source*, *Driver Model* and *Coexistence*. The *Angle Source* subsystem defines a driver angle demand signal δ_{D} that is assembled by a ramp profile, a quadratic polynomial profile and an exponential profile (the exponential profile is given by the analytical solution for the step response of a dynamical system with first order delay). Additionally, the driver deactivation flag F_{D} is given. If the flag is one, the “hands on” situation is active and vice versa. The driver deactivation flag is tuned for each vehicle manoeuvre such that the switching between the situations “hands on” to “hands off” or vice versa is valid for low lateral position errors and for no lane keeping assist torque interventions. In figure 6 the time signals for a lane keeping assist task are shown (the detailed steering manoeuvre description is found in the following chapter). The driver angle demand characterizes that the driver steers to -7.5° and releases the steering wheel. The driver deactivation flag drops from one to zero at the third second. The overlay torque T_{TO} is the lane keeping assist command signal in steering column coordinates. Figure 7 compares the steering wheel angle δ_{S} with the driver angle demand δ_{D}.

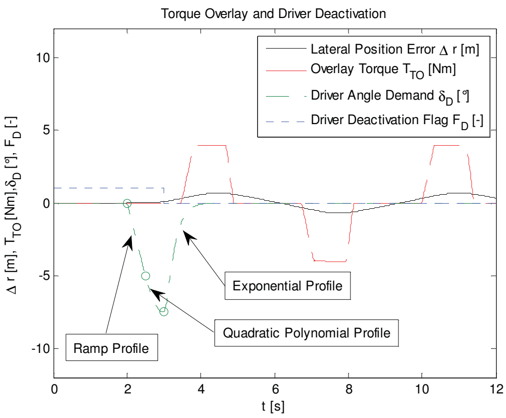

Figure 6. Time plots of the lateral position error (at the centre of gravity), overlay torque, driver angle demand, driver deactivation flag for the lane keeping assist task.

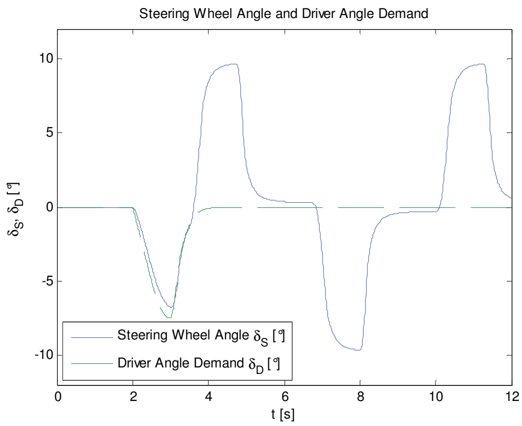

Figure 7. Time plots of the steering wheel angle and the driver angle demand for the lane keeping assist task.

Figure 8 shows the *Driver Model* subsystem that determines the driver as a controller in dependence on the driver angle demand δ_{D} and the steering wheel velocity $\dot{\delta}_{\mathrm{S}}$. The output of the *Driver Model* subsystem is the driver torque demand T_{DTD} which is weighted in the *Coexistence* subsystem that means the demand signal T_{DTD} is ramped up and down in dependence on the driver deactivation flag F_{D}.

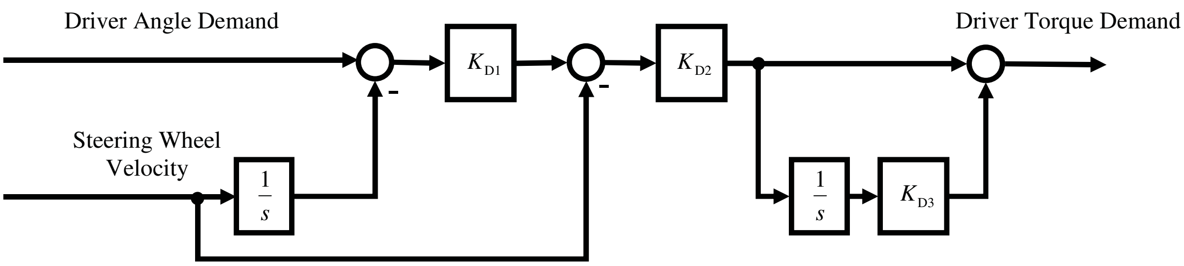

Figure 8. *Driver Model* of the situation model.

In figure 9 the driver torque T_{D} and the driver deactivation flag F_{D} are demonstrated. In figure 10 the driver torque demand T_{DTD} is additionally shown. The driver torque T_{D} represents exactly the driver torque demand T_{DTD} until the third second. Starting at the third second, the driver torque T_{D} is ramped down linearly due to fact that the situation “hands off” is detected. The driver torque demand T_{DTD} still gives an output signal from the driver model but this is not considered for the situation “hands off”. Simulating the lane keeping assist task with the trapezoid overlay torque approach requires the appropriate driver interaction modeling in the situation model as described in the figure 6-8. For the second control approach, the continuous operating lane guidance controller, the situation model reads very simple due to the fact that the situation “hands off” is modeled only. This means that the driver torque T_{D} in eq. (12) is zero for the whole simulation time.

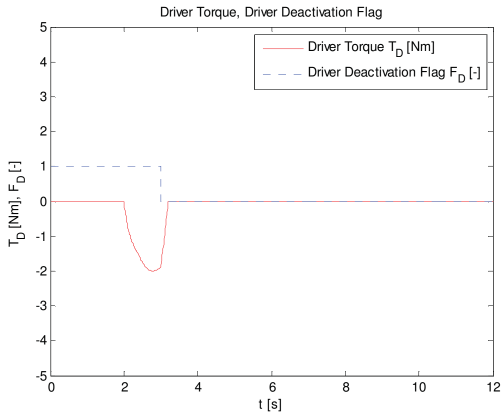

Figure 9. Time plots of the driver torque and the driver deactivation flag for the lane keeping assist task.

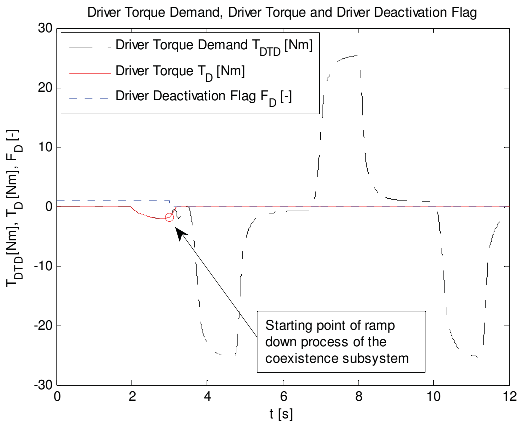

Figure 10. Time plots of the driver torque demand, driver torque and the driver deactivation flag for the lane keeping assist task.

3 Simulation results of lane keeping

The simulation study is carried out with a vehicle speed v_x of 70 km/h. For the lane keeping assist task the electric motor torque T_{EM} in eq. (11) provides the overlay torque. This overlay torque can be evaluated by two control approaches. The first approach determines a trapezoid overlay torque and the second approach a continuous operating lane guidance control torque. The first approach computes the electric motor torque T_{EM} in a lookup table in dependence on the lateral position error Δr. The lateral position error (shown in figure 2) is computed by

$$\Delta r = \frac{1}{s} v_x \left(\psi_R - \beta \right) \tag{13}$$

where ψ_R is called relative yaw angle or heading angle. The heading angle is further computed by the difference from the road tangent angle of the road reference trajectory and the vehicle yaw angle. Alternatively, the lateral position error can be computed by formulations given e.g. in [6]. The second approach makes use of a lane guidance controller similar to the one in [4]. Such a lane guidance controller is a cascaded controller with the input control signals as the road curvature κ, the lateral position error Δr_{pr} in a predefined preview distance l_{pr} and the heading angle ψ_R or the course angle $\nu = \psi + \beta$. The lateral position error Δr_{pr} in a predefined preview distance (shown in figure 2) can be formulated for small heading angles by

$$\Delta r_{pr} \approx \Delta r + l_{pr} \psi_R \, . \tag{14}$$

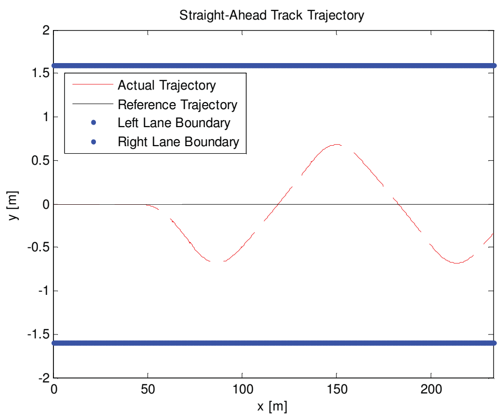

Figure 11. Bird's eye view of the vehicle for the trapezoid overlay torque: actual and reference trajectory, left and right lane boundaries.

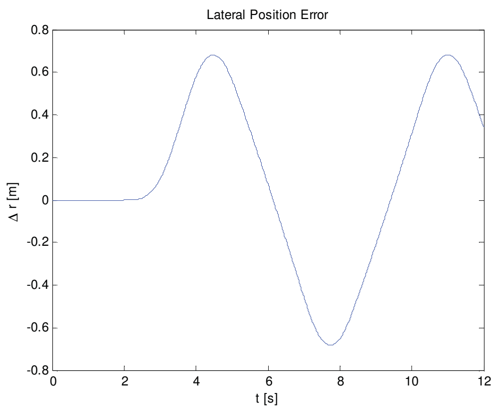

Figure 12. Time plot of the lateral position error (at the centre of gravity) for the trapezoid overlay torque.

In figure 11 the bird's eye view of the path of the vehicle for a straight-ahead road track is demonstrated. The driver steers for the first time towards the lane marking and releases then the steering wheel. It can be seen that the trapezoid overlay torque pushes the vehicle back to the road centre line. The torque overlay interaction appears three times and it is executed if the lateral position error reaches a certain deadband. The lateral position error (at the centre of gravity of the vehicle) is shown in figure 12.

In figure 13 and 14 the yaw angle and lateral acceleration of the vehicle are demonstrated. It is clearly shown that the vehicle remains in the linear region in terms of the vehicle dynamics.

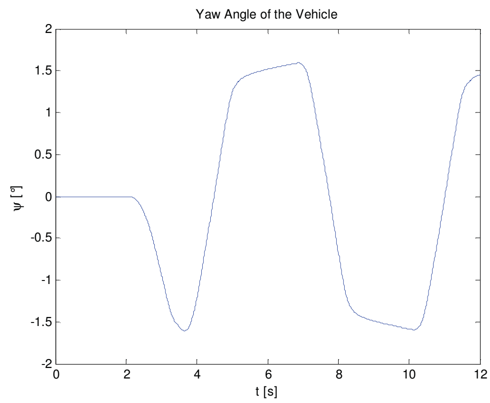

Figure 13. Time plot of the vehicle yaw angle for the trapezoid overlay torque.

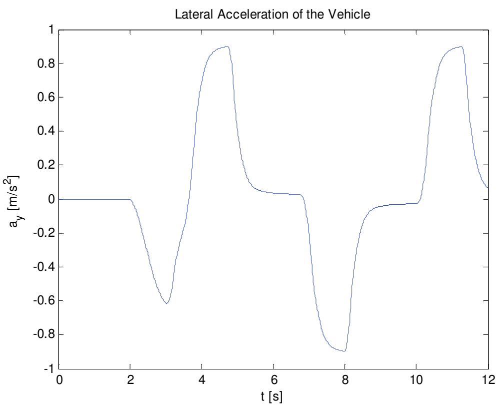

Figure 14. Time plot of the lateral acceleration for the trapezoid overlay torque.

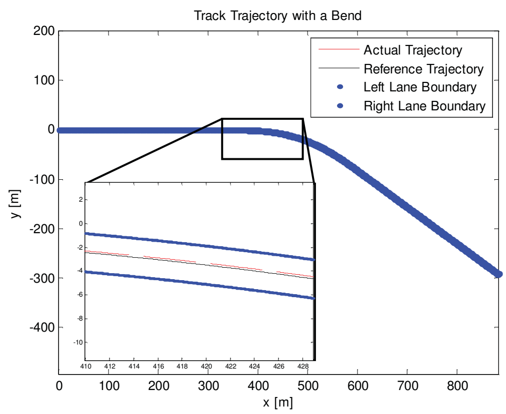

Figure 15. Bird's eye view of the vehicle for the continuous operating lane guidance controller: actual and reference trajectory, left and right lane boundaries.

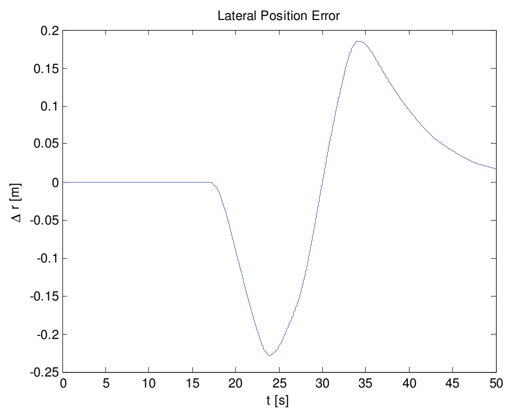

Figure 16. Time plot of the lateral position error (at the centre of gravity) for the continuous operating lane guidance controller.

Figure 15 shows the bird's eye view of the path of the vehicle for a road track with a straight-ahead part, a clothoid part, a bend part, a clothoid part and finally a straight-ahead part again.

Clothoids are mathematically defined by the track length s and the track length depends on the radius $R = 1/\kappa$ and the clothoid parameter A

$$s = \frac{A^2}{R}. \tag{15}$$

The x- and y-coordinate for the reference road trajectory are computed by the Fresnel integrals

$$x = \sqrt{\pi} A \cdot C(g) = \sqrt{\pi} A \cdot \int_0^g \cos\left(\frac{\pi}{2} v^2\right) \mathrm{d}v, \tag{16}$$

$$y = \sqrt{\pi} A \cdot S(g) = \sqrt{\pi} A \cdot \int_0^g \sin\left(\frac{\pi}{2} v^2\right) \mathrm{d}v. \tag{17}$$

The exact parameters for the road track composition are given in table 1.

Segment Number	Length [m]	Clothoid Starting Radius [m]	Clothoid Ending Radius [m]	Curvature Orientation	Clothoid Parameter [m]	Segment Type
1	330.555	∝	∝	-	-	SA
2	114.083	∝	300	negative	185	CSC
3	77.777	300	300	negative	-	C
4	114.083	300	∝	negative	185	CCS
5	500	∝	∝	-	-	SA

Table 1. Parameter definition of segments for the track with a bend (SA=Straight Ahead, CSC=Clothoid Straight Ahead to Circle, CCS=Clothoid Circle to Straight Ahead, C=Circle).

The continuous operating lane guidance controller works without a deadband in terms of the lateral position error. Although the radius of the bend reaches 300 m the lane guidance controller is capable to deal with lateral position errors (at the centre of gravity of the vehicle) less than 0.3 m which is a fair value (see figure 16). The yaw angle ψ of the vehicle in figure 17 and the curvature κ in figure 18 show the lane guidance performance and the road track composition.

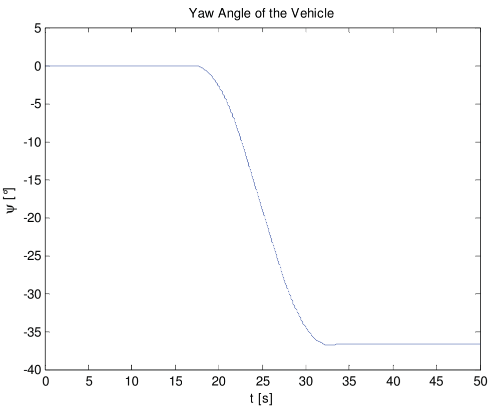

Figure 17. Time plot of the vehicle yaw angle for the continuous operating lane guidance controller.

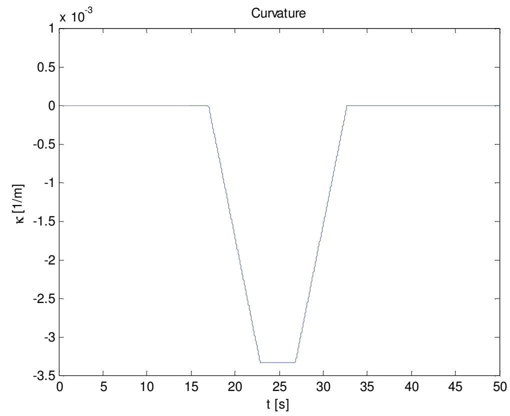

Figure 18. Time plot of the curvature for the continuous operating lane guidance controller.

4 Summary

Driver assistance systems and especially the lane keeping assist task contribute to safer vehicles and to more comfort for the driver. A demanding challenge is to model the different lane keeping assist control approaches regarding the mathematical interaction of a driver model in dependence on the situation if the driver does actively steer or not. The vehicle is modeled in this contribution as a bicycle model with two degrees of freedom (side slip angle and yaw angle) and the electro-hydraulic power assist rack and pinion steering gear is modeled with two degrees of freedom (rack position and steering wheel angle). The external rack force couples the vehicle model and the steering model. An electric motor mounted to the steering column of the vehicle provides the overlay torque for the lane keeping assist task. The lane keeping assist task can be introduced to the driver as a trapezoid overlay torque or as a continuous operating lane guidance controller. The results from a simulation study show the comparison of the two approaches. The trapezoid overlay torque approach shows that the vehicle is pushed back to the road centre line adequately if the lane boundary is reached. The lane guidance controller approach is capable to deal without a lateral position error deadband and to deal with higher bend radii.

5 References

[1] M. Börner. Modellierung, Analyse und Simulation der Fahrzeugquerdynamik. In: Fahrdynamik-Regelung: Modellbildung, Fahrerassistenzsysteme, Mechatronik (Ed.: R. Isermann). Vieweg, Wiesbaden. 2006.

[2] M. Bröcker. New Control Algorithms for Steering Feel Improvements of an Electric Powered Steering System with Belt Drive. In: Proceedings of the 19th Symposium of the international association for vehicle sys-

tem dynamics (Ed.: S. Bruni, G. Mastinu). Supplement to the International Journal of Vehicle System Dynamics. Volume 44. Taylor & Francis Group, Dorchester. 2006, 759-769.

[3] M. Mitschke, H. Wallentowitz. *Dynamik der Kraftfahrzeuge*. Springer, Berlin 2004.

[4] T. Müller, D. Rohleder. Automatisches Spurfahren auf Autobahnen. In: Fahrdynamik-Regelung: Modellbildung, Fahrerassistenzsysteme, Mechatronik (Ed.: R. Isermann). Vieweg, Wiesbaden. 2006.

[5] P. Riekert, T. E. Schunck. Zur Fahrmechanik des gummibereiften Kraftfahrzeugs. Ingenieur Archiv, Berlin 1940.

[6] R. S. Sharp, D. Casanova, P. Symonds. *A Mathematical Model for Driver Steering Control, with Design, Tuning and Performance.* Journal of Vehicle System Dynamics. Volume 33. Taylor & Francis Group, Dorchester. 2000, 289-326.

[7] J. P. Switkes, E. J. Rossetter, I. A. Coe, J. C. Gerdes. *Handwheel Force Feedback for Lane Keeping Assistance: Combined Dynamics and Stability.* Journal of Dynamic Systems, Measurement and Control. Volume 128. American Society of Mechanical Engineers, New York. 2006, 532-542.